

Heavy and light meson wavefunctions

Xing-Gang Wu*

Department of Physics, Chongqing University, Chongqing 401331, P.R. China

Tao Huang†

*Institute of High Energy Physics and Theoretical Physics Center for Science Facilities,
Chinese Academy of Sciences, Beijing 100049, P.R. China*

(Dated: October 15, 2018)

We present a short review on the properties of heavy and light mesons' light-cone wavefunctions (LCWFs), and their distribution amplitudes (DAs). The B meson LCWFs can be treated by taking the heavy quark limit ($m_b \rightarrow \infty$) and by using the heavy quark effective theory. Furthermore, we propose a simple model for the B meson WFs with 3-particle Fock states' contributions, whose behaviors are controlled by two parameters $\bar{\Lambda}$ and δ . Using such model, the form factors $F_{+,0,T}^{B \rightarrow \pi}$ and $F_{+,0,T}^{B \rightarrow K}$ in large recoil region are studied up to $\mathcal{O}(1/m_b^2)$ within the k_T factorization approach. On the other hand, we adopt Brodsky-Huang-Lepage (BHL) prescription for constructing the WFs of the lighter pseudoscalars as η_c , D-meson, pion, kaon, $\eta^{(\prime)}$ and etc. Such BHL-like model can be conveniently extended to construct the LCWFs for light scalar or vector mesons. Within such model the longitudinal distributions of those WFs are basically determined by a parameter B , whose value can be determined via a global fit of experimental data.

I. INTRODUCTION

The hadronic light-cone wavefunctions (LCWFs) exhibit all properties of the bound state and provide underlying links between the hadronic phenomena at large and small distances [1]. They are universal physical quantities for applying pQCD to exclusive processes. The study of phenomenology of hadronic LCWFs is an essential task to understand QCD dynamics, especially to understand the QCD factorization theory. Right now, we have not enough knowledge to determine the hadron LCWFs or their distribution amplitudes (DAs). The nonperturbative models such as AdS/QCD and light-front holography may provide a solution, a very recent review of which can be found in Ref.[2]. Practically, one can study their properties under some approximations/prescriptions or via a global fit of known experimental processes.

The B meson LCWFs can be treated by taking the heavy quark limit, $m_b \rightarrow \infty$, and by using the heavy quark effective theory (HQET) [3–5]. The B meson DAs and WFs have been investigated by various approaches [6–22]. Refs.[19–22] present an analytic solution for the B meson WFs $\Psi_{\pm}(\omega, z^2)$ up to next-to-leading order in Fock state expansion, which satisfies the constraints from the QCD equations of motion and the heavy-quark symmetry [23–25]. Under the Wandzura-Wilczek (WW) approximation [26], which corresponds to valence quark distribution only, the B meson WFs can be determined uniquely in terms of the “effective mass” ($\bar{\Lambda}$) and its transverse momentum dependence behaves simply as a δ -function. Such transverse momentum distribution can be considerably broadened by including the

3-particle Fock states' contributions. In the present paper, we shall review the properties of B meson WFs/DAs derived under HQET, whose parameters can be further constrained through a comparative study of $B \rightarrow \pi/K$ transition form factors (TFFs) derived under various approaches, such as pQCD, QCD light-cone sum rules (LC-SRs) and lattice QCD, or by a comparison of theoretical estimations with the experimental data on B decays.

For the light mesons as π , K , $\eta^{(\prime)}$ and etc., one can adopt the Brodsky-Huang-Lepage (BHL) prescription [27–29] together with the Wigner-Melosh rotation effect [30] to construct a reliable model for their WFs. This is the so-called revised light-cone harmonic oscillator model. The BHL prescription is obtained in a way by connecting the equal-time WF in the rest frame and the WF in the infinite momentum frame. Because of Wigner-Melosh rotation, there are higher-order helicity components for the WFs. Even though these higher helicity components are usually power suppressed in large energy region, they shall lead to sizable contributions in low and intermediate energy regions. It has been observed that the introduction of higher helicity components into the light-cone formalism shall result in significant consequence in several problems concerning the applicability of perturbative QCD, such as the pion and kaon electromagnetic form factors [31–35], the pion-photon TFF [36–45], and etc.. It has been found that by a proper change of input parameters, especially the value of B that basically determines the longitudinal behavior of the light meson WFs, one can conveniently simulate the shape of the light meson's DA from asymptotic-like [1] to CZ-like [46]. Thus, it provides a convenient way to compare the estimates with different DA behaviors. That is, by comparing the theoretical estimations with the corresponding experimental data, those undetermined parameters and hence its DA behavior can be fixed or at least be greatly restricted.

* wuxg@cqu.edu.cn

† huangtao@ihep.ac.cn

For the lighter mesons involving charm quark as compared to the B meson, i.e. the charmonium η_c or J/ψ and the D meson, the conditions are quite different from the case of B meson, since the charm quark is not heavy enough [15, 47–57]. We can construct their WFs in a similar way as that of light mesons. For example, it has been shown [52] that one can obtain a reliable LCSRs estimation for exclusive process $e^+ + e^- \rightarrow J/\psi + \eta_c$ by using a realistic η_c DA. That is, a proper η_c DA at a certain energy scale can result in a compatible prediction with the Belle and BaBar experimental data [51, 52]. Furthermore, it is noted that a proper way of constructing the D meson WF with a better end-point behavior at small longitudinal and transverse distribution region is very important for dealing with high energy processes such as $D \rightarrow \pi l \nu$ and $B \rightarrow D l \nu$. Especially, the $B \rightarrow D l \nu$ process can be further used to derive the value of $|V_{cb}|$ [58–60]. In the present paper, we shall discuss the η_c and D-meson WFs/DAs in detail, and present some of their

applications.

The remaining parts of the paper are organized as follows. In Sec.II, we give a brief review on the properties of heavy and light mesons' LCWFs. In Sec.III, we show some of their typical applications, i.e. the $B \rightarrow \pi$ TFFs, the determination of $|V_{cb}|$ and the light meson-photon TFFs. The final section is reserved for a summary and outlook.

II. PROPERTIES OF THE MESON WAVEFUNCTIONS

A. B meson WFs

In HQET, the B meson WFs $\tilde{\Psi}_{\pm}(t, z^2)$ can be defined in terms of the vacuum-to-meson matrix element of the nonlocal operators [61]:

$$\langle 0 | \bar{q}(z) \Gamma h_v(0) | \bar{B}(p) \rangle = -\frac{if_B M}{2} \text{Tr} \left[\gamma_5 \Gamma \frac{1 + \not{v}}{2} \times \left\{ \tilde{\Psi}_+(t, z^2) - \not{z} \frac{\tilde{\Psi}_+(t, z^2) - \tilde{\Psi}_-(t, z^2)}{2t} \right\} \right], \quad (1)$$

where $z^\mu = (0, z^-, \mathbf{z}_\perp)$, $z^2 = -\mathbf{z}_\perp^2$, $v^2 = 1$, $t = v \cdot z$ and $p^\mu = Mv^\mu$ is the B meson 4-momentum with mass M , $h_v(x)$ denotes the effective b -quark field and Γ is a generic Dirac matrix. The path-ordered gauge factors are implied between constituent quark fields. After doing the Fourier transformation, we have $\tilde{\Psi}_{\pm}(t, z^2) \rightarrow \Psi_{\pm}(\omega, z^2)$. The B meson DAs can be obtained by taking the LC limit to the B meson WFs, i.e. $\phi_{\pm}(\omega) \equiv \lim_{z^2 \rightarrow 0} \Psi_{\pm}(\omega, z^2)$.

1. B meson WFs in WW approximation

The equation of motion of the light spectator quark imposes a strong constraint on the B meson WFs. When ignoring the 3-particle Fock states' contributions, one obtains the WW-type B meson WFs. In this case, their DAs are [19, 21]:

$$\phi_+^{WW}(\omega) = \frac{\omega}{2\bar{\Lambda}^2} \theta(\omega) \theta(2\bar{\Lambda} - \omega), \quad (2)$$

$$\phi_-^{WW}(\omega) = \frac{2\bar{\Lambda} - \omega}{2\bar{\Lambda}^2} \theta(\omega) \theta(2\bar{\Lambda} - \omega), \quad (3)$$

where $\bar{\Lambda} = \frac{iv \cdot \partial \langle 0 | \bar{q} \Gamma h_v | \bar{B}(p) \rangle}{\langle 0 | \bar{q} \Gamma h_v | \bar{B}(p) \rangle}$ is the B meson "effective mass". $\theta(\omega)$ is the unit step function, $\theta(\omega) = 0$ for $\omega < 0$ and $\theta(\omega) = 1$ for $\omega \geq 0$. The transverse part of the B meson WFs is a zero-th normal Bessel function [21]. More explicitly, after applying Fourier transformation,

$$\tilde{\Psi}_{\pm}(\omega, \mathbf{k}_\perp) = \int \frac{d^2 \mathbf{z}_\perp}{(2\pi)^2} \exp(-i \mathbf{k}_\perp \cdot \mathbf{z}_\perp) \Psi_{\pm}(\omega, z^2),$$

the WW WFs can be written as

$$\tilde{\Psi}_+^{WW}(\omega, \mathbf{k}_\perp) = \frac{\phi_+^{WW}(\omega)}{\pi} \delta(\mathbf{k}_\perp^2 - \omega(2\bar{\Lambda} - \omega)), \quad (4)$$

$$\tilde{\Psi}_-^{WW}(\omega, \mathbf{k}_\perp) = \frac{\phi_-^{WW}(\omega)}{\pi} \delta(\mathbf{k}_\perp^2 - \omega(2\bar{\Lambda} - \omega)). \quad (5)$$

This indicates that the transverse dependence of the B meson WW WF behaves as a δ -function and the WFs' dependence on the transverse and longitudinal momenta is strongly correlated via a combined variable $\mathbf{k}_\perp^2 / [\omega(2\bar{\Lambda} - \omega)]$. This off-shell-energy-like transverse dependence has also been observed by using the dispersion relation and the quark-hadron duality [62], which in some sense is consistent with the BHL idea for the light meson WFs.

2. B meson WFs in 3-particle Fock states

To get the B meson WFs $\Psi_{\pm}(\omega, z^2)$ including the 3-particle Fock states, one needs to know the transverse properties of the 3-particle WFs [19, 20, 22]: $\Psi_V(\rho, \xi, z^2)$, $\Psi_A(\rho, \xi, z^2)$, $X_A(\rho, \xi, z^2)$ and $Y_A(\rho, \xi, z^2)$. An approximate solution for $\Psi_{\pm}(\omega, z^2)$ including the 3-particle Fock states can be obtained by taking the assumptions:

I) The final $\Psi_{\pm}(\omega, z^2)$ have the same transverse momentum dependence, i.e.

$$\Psi_{\pm}[\omega, z^2] = \phi_{\pm}(\omega) \chi[\omega, z^2], \quad (6)$$

and all 3-particle WFs have the same transverse momentum dependence $\chi^{(h)}(\rho, \xi, z^2)$, i.e.

$$\Psi_A(\rho, \xi, z^2) = \Psi_A(\rho, \xi) \chi^{(h)}(\rho, \xi, z^2), \quad (7)$$

$$\Psi_V(\rho, \xi, z^2) = \Psi_V(\rho, \xi) \chi^{(h)}(\rho, \xi, z^2), \quad (8)$$

$$X_A(\rho, \xi, z^2) = X_A(\rho, \xi) \chi^{(h)}(\rho, \xi, z^2), \quad (9)$$

$$Y_A(\rho, \xi, z^2) = Y_A(\rho, \xi) \chi^{(h)}(\rho, \xi, z^2), \quad (10)$$

with the boundary condition $\lim_{z^2 \rightarrow 0} \chi^{(h)}(\rho, \xi, z^2) = 1$.

II) It is noted that main features of the 3-particle DAs are dominated by its first several moments, then one can assume that the relation among the first non-zero double moments of the 3-particle DAs are also satisfied by the 3-particle DAs themselves, e.g.

$$Y_A(\rho, \xi) \simeq \frac{X_A(\rho, \xi) - 3\Psi_A(\rho, \xi)}{4}. \quad (11)$$

III) The difference between $\Psi_V(\rho, \xi)$ and $\Psi_A(\rho, \xi)$ satisfies the relation [12],

$$\Psi_V(\rho, \xi) - \Psi_A(\rho, \xi) = \frac{\lambda_H^2 - \lambda_E^2}{6\bar{\Lambda}^5} \rho \xi^2 \exp\left(-\frac{\rho + \xi}{\bar{\Lambda}}\right), \quad (12)$$

where λ_E and λ_H are matrix elements of chromoelectric and chromomagnetic fields in B meson rest frame.

With those assumptions, one can obtain the normalized transverse distributions for the B meson WFs, which when transformed into the \mathbf{k}_\perp space takes the following form [22]:

$$\tilde{\chi}(\omega, \mathbf{k}_\perp) = - \left(\frac{1}{\Gamma[1 - c_1]\pi} + \frac{\Gamma[2 - c_1] \sin[\pi c_1]}{\pi^2} K_2 \right) \frac{\Gamma[2 - c_1]}{((2\bar{\Lambda} - \omega)\omega) \left| 1 - \frac{k_T^2}{(2\bar{\Lambda} - \omega)\omega} \right|^{2 - c_1}}, \quad (13)$$

$$\Psi_+(\omega, b) = \frac{\omega}{\omega_0^2} \exp\left(-\frac{\omega}{\omega_0}\right) \left(\Gamma[\delta] J_{\delta-1}[\kappa] + (1 - \delta) \Gamma[2 - \delta] J_{1-\delta}[\kappa] \right) \left(\frac{\kappa}{2} \right)^{1-\delta}, \quad (15)$$

$$\Psi_-(\omega, b) = \frac{1}{\omega_0} \exp\left(-\frac{\omega}{\omega_0}\right) \left(\Gamma[\delta] J_{\delta-1}[\kappa] + (1 - \delta) \Gamma[2 - \delta] J_{1-\delta}[\kappa] \right) \left(\frac{\kappa}{2} \right)^{1-\delta}, \quad (16)$$

where $\omega_0 = 2\bar{\Lambda}/3$, $\kappa = \sqrt{\omega(2\bar{\Lambda} - \omega)}b$, $\delta \in (0, 1)$ and $\lambda_E^2 \simeq \lambda_H^2 \simeq 2\bar{\Lambda}^2/3$ is adopted. The range of ω is fixed within the range of $(0, 2\bar{\Lambda})$. When $\delta \rightarrow 1$, the transverse momentum dependence of the B meson WF returns to that of the WW-like B meson WF.

B. Lighter meson WFs

In this subsection, we sequentially present the leading-twist WFs for several typical lighter mesons, such as pion, η_c , kaon and D meson, respectively. We construct the WFs based on the BHL prescription. Because of the Wigner-Melosh rotation [30], as a sound estimation, one also has to take the higher-order helicity components into consideration to construct the WF. As a subtle point, it is noted that such idea of constructing the light meson

where K_2 is an input parameter, $c_1 \in (0, 1)$ and $k_T = |\mathbf{k}_\perp|$. It indicates that the B meson WF may be expanded to a hyperbola-like curve rather than a simple WW-like δ -function. As an example, we put the transverse distributions of $\tilde{\chi}(\omega, \mathbf{k}_\perp)$ with fixed $\bar{\Lambda} = 0.55$ GeV and $\omega = 0.5$ GeV in Fig.(1).

As for the B meson DAs $\phi_\pm(\omega)$, they have a quite complex form by considering the higher Fock state into consideration. By using the approximation, $\lambda_E^2 \simeq \lambda_H^2 \simeq 2\bar{\Lambda}^2/3$, they have the following simpler forms,

$$\phi_+(\omega) = \frac{\omega}{\omega_0^2} \exp\left(-\frac{\omega}{\omega_0}\right), \quad \phi_-(\omega) = \frac{1}{\omega_0} \exp\left(-\frac{\omega}{\omega_0}\right), \quad (14)$$

where $\omega_0 = 2\bar{\Lambda}/3$. The $\phi_\pm(\omega)$ agrees well with the model raised by Ref.[61] within a QCD sum rule analysis.

3. A simple model for B meson WFs

To be more applicable, we propose a simple model for the B meson WFs with 3-particle Fock states' contributions. For convenience, we write the normalized B meson WFs in the compact parameter b -space (especially useful for the k_T -factorization approach [63–66]):

WFs can be conveniently extended to scalar or vector mesons, or to higher twist WFs. For example, the twist-3 WFs for pion and kaon following the same spirit can be found in Refs.[34, 35].

$$\chi^{\lambda_1 \lambda_2}(x, \vec{k}_\perp) = \frac{\lambda_1 \lambda_2}{\sqrt{2} m_{qT}} \begin{array}{cccc} \uparrow\uparrow & \uparrow\downarrow & \downarrow\uparrow & \downarrow\downarrow \\ -\frac{k_x - ik_y}{\sqrt{2} m_{qT}} & \frac{m_q}{\sqrt{2} m_{qT}} & -\frac{m_q}{\sqrt{2} m_{qT}} & -\frac{k_x + ik_y}{\sqrt{2} m_{qT}} \end{array}$$

TABLE I. Pion spin-space WF $\chi^{\lambda_1 \lambda_2}(x, \vec{k}_\perp)$, where $\vec{k}_\perp = (k_x, k_y)$ and m_q stands for the light constituent quark mass. The transverse mass $m_{qT} = \sqrt{m_q^2 + k_\perp^2}$.

Firstly, based on the BHL prescription, the pion leading-twist WF can be constructed as [36–42]

$$\Psi_\pi(x, \mathbf{k}_\perp) = \sum_{\lambda_1 \lambda_2} \chi^{\lambda_1 \lambda_2}(x, \mathbf{k}_\perp) \Psi_\pi^R(x, \mathbf{k}_\perp), \quad (17)$$

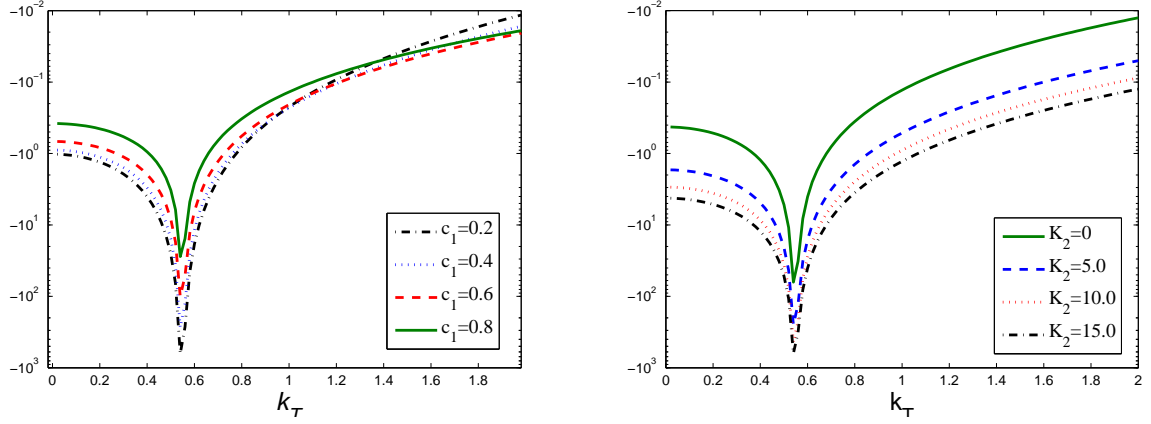


FIG. 1. The normalized transverse distribution $\tilde{\chi}(\omega, \mathbf{k}_\perp)$ ($k_T = |\mathbf{k}_\perp|$) with $\bar{\Lambda} = 0.55$ GeV and $\omega = 0.5$ GeV [22]. The left diagram is for $K_2 = 1$ with $c_1 = 0.2, 0.4, 0.6$ and 0.8 , respectively; while the right diagram is for $c_1 = 0.6$ with $K_2 = 0, 5.0, 10.0$ and 15.0 , respectively.

where $\chi^{\lambda_1\lambda_2}(x, \mathbf{k}_\perp)$ stands for the spin-space WF, λ_1 and λ_2 being the helicity states of the two constitute quarks in pion. The $\chi^{\lambda_1\lambda_2}(x, \mathbf{k}_\perp)$ comes from Wigner-Melosh rotation [30], whose explicit forms are presented in Table I. $\Psi_\pi^R(x, \mathbf{k}_\perp)$ indicates the spatial WF, whose \mathbf{k}_\perp -dependent part can be constructed by using the connection between the rest frame WF $\Psi_{c.m.}(\mathbf{q})$ and the LCWF $\Psi_{LC}(x, \mathbf{k}_\perp)$, i.e.

$$\Psi_{c.m.}(\mathbf{q}^2) \longleftrightarrow \Psi_{LC} \left[\frac{\mathbf{k}_\perp^2 + m_q^2}{4x(1-x)} - m_q^2 \right], \quad (18)$$

where $m_q \sim 0.3$ GeV stands for the mass of the light constitute quarks of pion. As for the pure x -dependent part of $\Psi_\pi^R(x, \mathbf{k}_\perp)$, we take $\varphi_\pi(x) = [1 + B_\pi \times C_2^{3/2}(2x-1)]$ with $B_\pi \sim a_\pi^2$, which dominates the WF longitudinal distribution. Then, the full form of the spatial WF can be obtained,

$$\Psi_\pi^R(x, \mathbf{k}_\perp) = A_\pi \varphi_\pi(x) \exp \left[-\frac{\mathbf{k}_\perp^2 + m_q^2}{8\beta_\pi^2 x(1-x)} \right], \quad (19)$$

where A_π is the overall normalization constant. After integrating over the transverse momentum dependence, one obtains the pion DA,

$$\phi_\pi(x, \mu_0^2) = \frac{\sqrt{3}A_\pi m_q \beta_\pi}{2\pi^{3/2} f_\pi} \sqrt{x(1-x)} \varphi_\pi(x) \times \left\{ \text{Erf} \left[\sqrt{\frac{m_q^2 + \mu_0^2}{8\beta_\pi^2 x(1-x)}} \right] - \text{Erf} \left[\sqrt{\frac{m_q^2}{8\beta_\pi^2 x(1-x)}} \right] \right\}, \quad (20)$$

where μ_0 is the factorization scale and $\text{Erf}(x)$ is the usual error function, $\text{Erf}(x) = \frac{2}{\sqrt{\pi}} \int_0^x e^{-t^2} dt$.

Two constraints can be adopted to constrain the pion WF: (1) the normalization condition

$$\int_0^1 dx \int \frac{d^2\mathbf{k}_\perp}{16\pi^3} \Psi_\pi(x, \mathbf{k}_\perp) = \frac{f_\pi}{2\sqrt{6}}; \quad (21)$$

(2) the sum rule derived from $\pi^0 \rightarrow \gamma\gamma$ decay amplitude

$$\int_0^1 dx \Psi_\pi(x, \mathbf{k}_\perp = \mathbf{0}) = \frac{\sqrt{6}}{f_\pi}, \quad (22)$$

where $f_\pi = 130.41 \pm 0.03 \pm 0.20$ MeV [67].

We put the pion WF parameters at the scale $\mu_0 = 1$ GeV in Table II. When $B_\pi \in [0.00, 0.60]$, such DA model can mimic the pion DA shapes from asymptotic-like [1] to CZ-like [46]. More explicitly, we put the DAs for $B_\pi = 0.00, 0.30$ and 0.60 in Fig. (2), where as a comparison, the asymptotic DA and CZ-DA have also been present. If we have precise measurements for certain processes, then by comparing the theoretical estimations, one can fix the pion DA behavior.

Moreover, the pion DA can be run into any other scales by applying the evolution equation, i.e. to order $\mathcal{O}(\alpha_s)$, we have [1]

$$x_1 x_2 \frac{\partial \tilde{\phi}_\pi(x_i, \mu^2)}{\partial \ln \mu^2} = C_F \frac{\alpha_s(\mu^2)}{4\pi} \times \left\{ \int_0^1 [dy] V(x_i, y_i) \tilde{\phi}_\pi(y_i, \mu^2) - x_1 x_2 \tilde{\phi}_\pi(x_i, \mu^2) \right\}, \quad (23)$$

B_π	$A_\pi(\text{GeV}^{-1})$	$\beta_\pi(\text{GeV})$	$a_2^\pi(\mu_0^2)$	$a_4^\pi(\mu_0^2)$
0.00	24.80	0.589	0.028	-0.027
0.30	20.05	0.672	0.364	-0.017
0.60	16.46	0.749	0.681	0.022

TABLE II. Pion WF parameters for $m_q = 0.30$ GeV [42]. The second and fourth Gegenbauer moments are also presented as an explanation of pion DA behavior. It shows $B_\pi \sim a_2^\pi$, which indicates that B_π dominantly determines the broadness of the longitudinal behavior of WF.

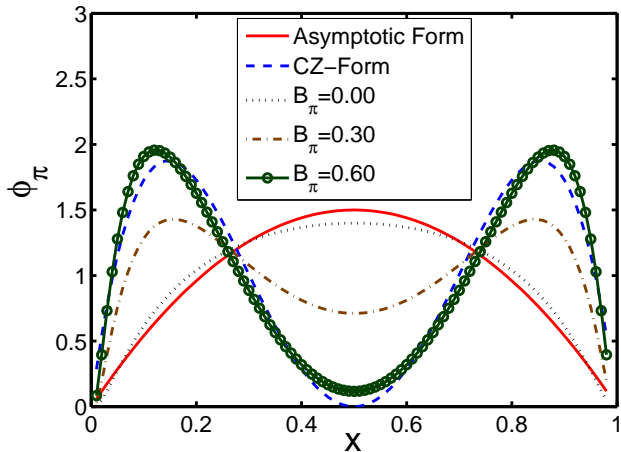


FIG. 2. The pion DA model $\phi_\pi(x, \mu_0^2)$ versus the parameter B_π [39]. By varying B_π from 0.00 to 0.60, $\phi_\pi(x, \mu_0^2)$ changes from asymptotic-like to CZ-like.

where $[dy] = dy_1 dy_2 \delta(1 - y_1 - y_2)$, $\phi_\pi(x_i, \mu^2) = x_1 x_2 \tilde{\phi}_\pi(x_i, \mu^2)$ and

$$V(x_i, y_i) = 2x_1 y_2 \theta(y_1 - x_1) \left(\delta_{h_1 \bar{h}_2} + \frac{\Delta}{(y_1 - x_1)} \right) + (1 \leftrightarrow 2).$$

The color factor $C_F = 4/3$, $\delta_{h_1 \bar{h}_2} = 1$ for opposite q and \bar{q} helicities, and $\Delta \tilde{\phi}_\pi(y_i, \mu^2) = \tilde{\phi}_\pi(y_i, \mu^2) - \tilde{\phi}_\pi(x_i, \mu^2)$. Practically, the above evolution (23) can be solved numerically or be solved by using the DA Gegenbauer expansion, which transforms the DA's scale dependence to the scale dependence of the Gegenbauer moments.

It is noted that, sometimes, a factor $1/x(1-x)$ or $\partial k_z / \partial x$ has also been introduced into the WF. It is noted that the factor $\partial k_z / \partial x$ comes from the transformation of the WF from the instant form to the light-cone form. The longitudinal component $k_z = (x-1/2)M_0$ with pion invariant mass $M_0 = \sqrt{(\mathbf{k}_\perp^2 + m_q^2)/x(1-x)}$. These factors only slightly change the end-point behavior from the BHL-like terms and we only need to change the WF parameters properly.

Secondly, the η_c WF can be obtained by applying the transition of $m_q \rightarrow m_c$ to Eq.(17). In addition to

the normalization condition, we can use the condition $P_{\eta_c} \simeq 0.8$ [30] to constrain the WF parameter, in which P_{η_c} stands for the probability of finding the leading Fock state $|c\bar{c}\rangle$ in the η_c Fock state expansion, i.e.

$$P_{\eta_c} = \int_0^1 dx \int \frac{d^2 k_\perp}{16\pi^3} |\Psi_{\eta_c}^R(x, \mathbf{k}_\perp)|^2. \quad (24)$$

We set $\mu_0 = m_c$ to be the initial scale for the non-perturbative distribution amplitude of the η_c -meson. For other choice of factorization scale, one can conveniently obtain its DA by using the above mentioned evolution equation (23). An example, by taking the constituent quark mass $m_c = 1.8$ GeV and the decay constant $f_{\eta_c} = 0.335$ GeV [67], we get $A_{\eta_c} = 286$ GeV $^{-1}$ and $\beta_{\eta_c} = 0.810$ GeV $^{-2}$ under the case of $B_{\eta_c} = 0$. We present its DA in Fig.(3), in which a comparison with those of Bondar-Chernyak (BC) model [48], Bodwin-Kang-Lee (BKL) model [68] and Braguta-Likhoded-Luchinsky

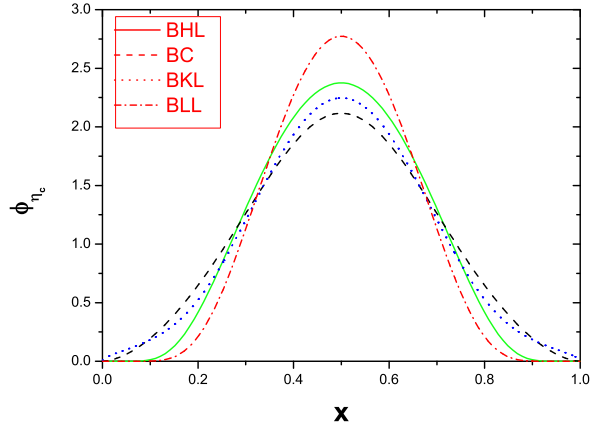


FIG. 3. A comparison of the η_c DA $\phi_{\eta_c}(x, \mu_0^2)$ [52] for $B_{\eta_c} = 0$ with those of the BC model [48], the BKL model [68] and the BLL model [69] at the initial scale $\mu_0 = m_c$.

$$\Psi_K^R(x, \mathbf{k}_\perp) = A_K [1 + B_K C_1^{3/2} (2x - 1) + C_K C_2^{3/2} (2x - 1)] \times \exp \left[-b_K^2 \left(\frac{k_\perp^2 + m_1^2}{x} + \frac{k_\perp^2 + m_2^2}{1-x} \right) \right]. \quad (25)$$

Here the pure x -dependent part $\varphi_K(x)$ has also been expanded in Gegenbauer expansion, i.e.,

$$\varphi_K(x) = [1 + B_K C_1^{3/2} (2x - 1) + C_K C_2^{3/2} (2x - 1)],$$

where $m_1 = m_u$ and $m_2 = m_s$ for K^+ , $m_1 = m_d$ and $m_2 = m_s$ for K^0 . The length of the non-zero Gegenbauer terms depends on how well we know the Gegenbauer moments. Some other models have also been suggested for kaon WF, c.f. Refs.[70, 71], which are (numerically) consistent with the present model.

Because of different constituent quarks, kaon meson has non-zero first Gegenbauer moment. In the literature, the first and second Gegenbauer moments a_1^K and a_2^K have been studied by several approaches with high precision, such as Refs. [72–83]. So we keep two Gegenbauer terms in $\varphi_K(x)$. The spin-space part χ_K is more complex than the pionic case due to different constituent quark masses, whose explicit form can be found in Ref.[35]. Four parameters A_K , B_K , C_K and b_K can be determined by its DA's first two Gegenbauer moments a_1^K and a_2^K , the constraint $(\mathbf{k}_\perp^2)_K^{1/2} \approx 0.350 \text{ GeV}$ [6] and the normalization condition. As an example, by taking $a_1^K(1 \text{ GeV}) = 0.05$ [75] and $a_2^K(1 \text{ GeV}) = 0.115$ [82, 83], we have $A_K = 12.55 \text{ GeV}^{-1}$, $B_K = 0.0605$, $C_K = 0.0348$ and $b_K = 0.8706 \text{ GeV}^{-1}$.

Fourthly, the D -meson WF $\Psi_D(x, \mathbf{k}_\perp)$ can be constructed in the same way as the kaon WF, i.e. for the present case, $m_1 = m_c$ and $m_2 = m_d$. Because $m_c \gg m_d$, we shall have large non-zero first Gegenbauer moment a_1^D . As a simplified treatment, we find

(BLL) model [69] has also been presented.

Thirdly, because the two constituent quarks are different, the leading-twist kaon WFs is slightly different from the case of pion. That is, the spatial part of the kaon WF $\Psi_K(x, \mathbf{k}_\perp) = \Psi_K^R(x, \mathbf{k}_\perp) \chi_K$ can be constructed as

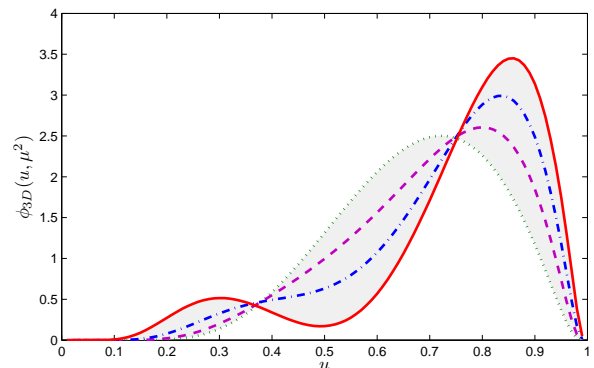


FIG. 4. The D meson DA $\phi_D(x, \mu_0^2)$ at $\mu_0 = 1 \text{ GeV}$ with different B_D [57]. The dotted, the dashed, the dash-dot and the solid lines are for $B_D = 0.00, 0.20, 0.40$ and 0.60 , respectively.

it is convenient to set the x -dependent part as $\varphi_D(x) = [1 + B_D \times C_2^{3/2} (2x - 1)]$ [57], in which the value of B_D is close to the second Gegenbauer moment, $B_D \sim a_2^D$, which basically determines the broadness of the longitudinal distribution. After integrating over the transverse momentum, we get the D meson DA. The parameter B_D is a free parameter for ϕ_D . As an example, we put the D meson DA ϕ_D with different B_D in Fig.(4), in which we have set $B_D = 0.00, 0.20, 0.40$ and 0.60 . By vary-

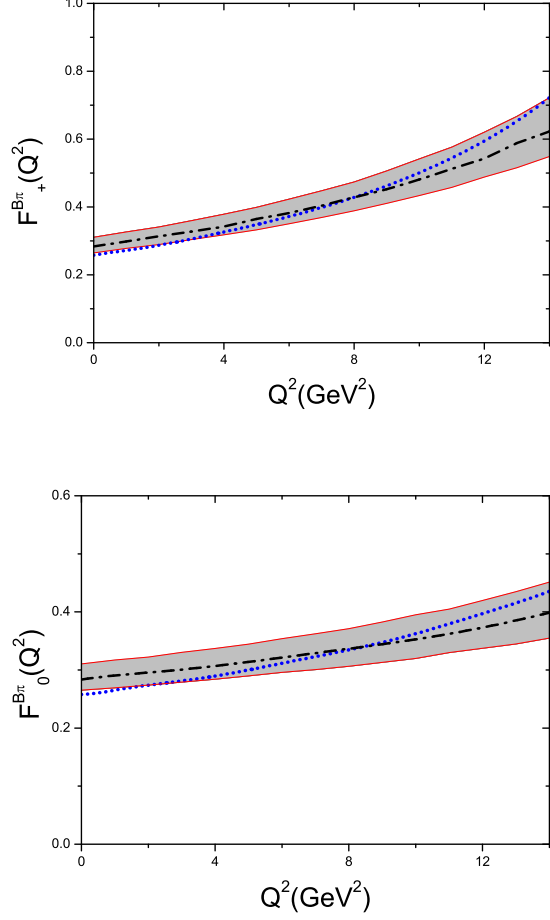


FIG. 5. The B meson TFFs $F_+^{B\pi}(Q^2)$ and $F_0^{B\pi}(Q^2)$ [22]. The upper (lower) edge of the shaded band is for $\delta = 0.30$ ($\delta = 0.25$), and the dash-dot line is for $\delta = 0.27$. The dotted line is for the estimation of LCSRs [82, 83]. $\bar{\Lambda} = 0.55$ GeV.

ing B_D within a certain region, e.g. $[0.00, 0.60]$, we can reproduce most of the D meson DAs suggested in the literature. For example, as $B_D = 0.00$, it corresponds to the D meson wave function suggested in Ref.[6]. It is noted that by setting $B_D \in [0.00, 0.40]$, we get the first Gegenbauer moment $a_1^D \sim [0.6, 0.8]$, which is consistent with those suggested in the literature, and the second Gegenbauer moment $a_2^D \sim B_D$.

III. APPLICATIONS

A. $B \rightarrow \pi$ transition form factors

Applying the WW B meson WFs, we have shown that the $B \rightarrow \pi$ transition form factors (TFFs) calculated by using the k_T -factorization approach are consistent with those of QCD LCSRs and lattice QCD approaches [84], which are applicable in different q^2 regions. Results of

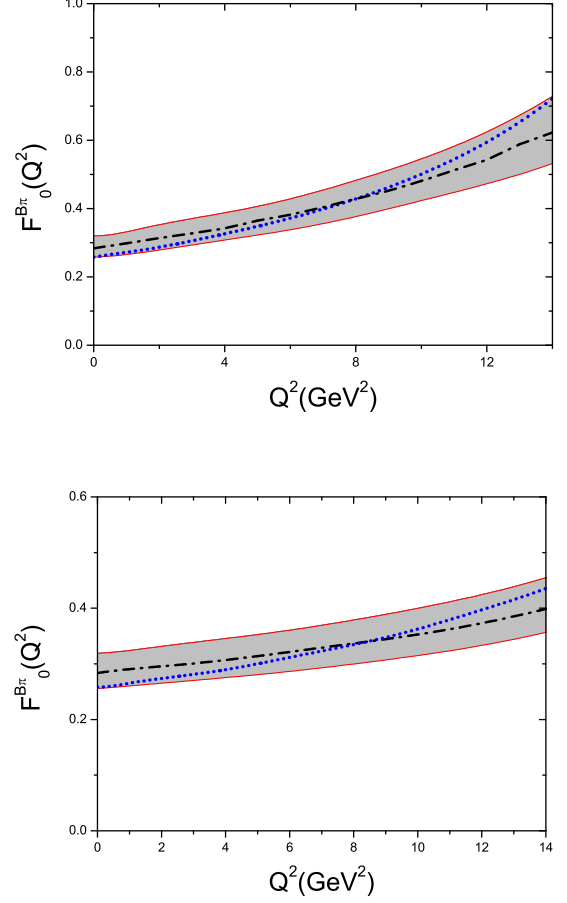


FIG. 6. The B meson TFFs $F_+^{B\pi}(Q^2)$ and $F_0^{B\pi}(Q^2)$ [22]. The upper (lower) edge of the shaded band is for $\bar{\Lambda} = 0.52$ GeV ($\bar{\Lambda} = 0.58$ GeV), the dash-dot line is for $\bar{\Lambda} = 0.55$ GeV. The dotted line is for the estimation of LCSRs [82, 83]. $\delta = 0.27$.

Ref.[84] indicates that

- The negative contribution from $\bar{\Psi}_B = \frac{\Psi_+ - \Psi_-}{2}$ is necessary to suppress the big contribution from $\Psi_B = \frac{\Psi_+ + \Psi_-}{2}$ so as to obtain a reasonable total contributions. Thus, the properties of $\bar{\Psi}_B$ and Ψ_B are important for an accurate estimation.
- A better PQCD result (with its slope closest to the QCD LCSR results) can be obtained by carefully considering both the pionic twist-3 contributions and the contributions from the B meson WFs $\bar{\Psi}_B$ and Ψ_B . The pionic twist-3 WFs constructed via a similar way of leading twist WF can effectively suppress the end-point singularity and lead to a reliable twist-3 contributions.

As suggested in Eqs.(15,16), by including 3-particle Fock states into B meson WFs, there are two unknown but universal parameters $\bar{\Lambda}$ and δ for the B meson WFs in compact parameter b -space. To see how the 3-particle

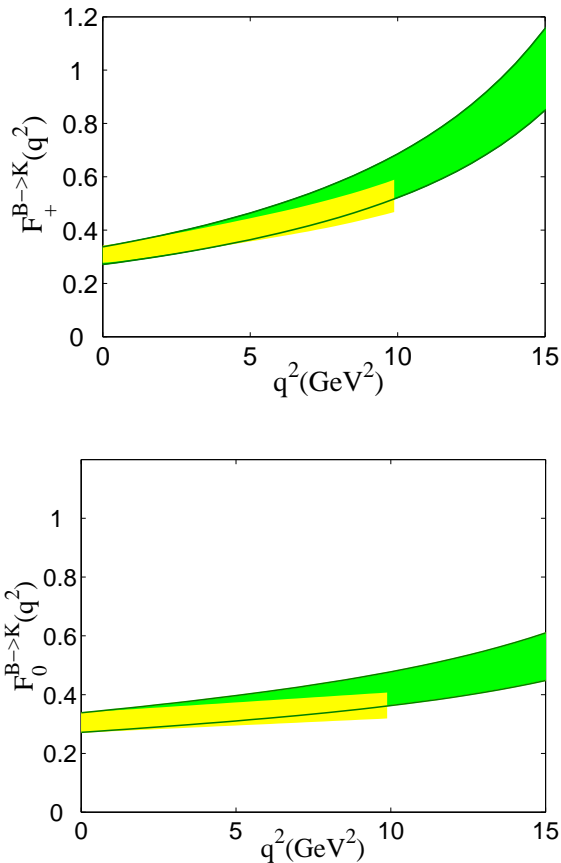


FIG. 7. A comparison of $F_{+,0}^{B \to K}(q^2)$ within the k_T factorization and the LCSR [85], where the lighter shaded band stands for k_T factorization results for $\delta \sim (0.25, 0.30)$ and $\bar{\Lambda} \sim (0.50 \text{ GeV}, 0.55 \text{ GeV})$, while, the thicker shaded band stands for LCSR results [82, 83].

Fock states affect the $B \rightarrow \pi$ TFFs, we calculate them within the k_T -factorization approach and show how $\bar{\Lambda}$ and δ affect the final estimations. Inversely, by comparing with the data, one can obtain reasonable regions for $\bar{\Lambda}$ and δ [85].

As a rough estimation, we show how the 3-particle Fock states affect the B meson decays. That is, a rough order estimation of $B \rightarrow \pi$ TFFs can be obtained by the first inverse moment of B meson DA $\phi_+(\omega)$, which satisfies

$$\Lambda_0 = \int \frac{d\omega}{\omega} \phi_+(\omega) = \frac{1}{\lambda_B}, \quad (26)$$

where $\lambda_B = 460 \pm 160 \text{ MeV}$ [12, 13]. One may find that $(\Lambda_0^{(g)}/\Lambda_0^{WW}) = (\bar{\Lambda} - \lambda_B)/\lambda_B \sim 0.2$ [22], where $\Lambda_0^{(g)}$ is the first inverse moment of $\phi_+^{(g)}(\omega)$ and Λ_0^{WW} is that of $\phi_+^{WW}(\omega)$. In Ref.[86], the 3-particle contributions are estimated by attaching an extra gluon to the internal off-shell quark line, and then $(1/m_b) \sim 0.2$ power suppression is readily induced.

By taking the B meson WFs as defined in Eqs.(15,16) and a comparison of the estimations under the k_T -

factorization and LCSR approaches, we make a discussion on the uncertainties of $B \rightarrow \pi$ TFF caused by δ and $\bar{\Lambda}$. To concentrate our attention on B meson WFs, we adopt the pion WF as that of Ref.[84]. We present the $B \rightarrow \pi$ TFFs $F_{+,0}^{B\pi}(Q^2)$ with fixed $\bar{\Lambda} = 0.55 \text{ GeV}$ in Fig.(5), while the cases with fixed $\delta = 0.27$ are shown in Fig.(6). Our results show that if the contribution from the 3-particle wavefunction is limited to be within $\pm 20\%$ of that of WW wavefunction with $Q^2 \in (0, \sim 10 \text{ GeV}^2)$, then the possible range of δ and $\bar{\Lambda}$ are, $\delta \sim (0.25, 0.30)$ and $\bar{\Lambda} \sim (0.50 \text{ GeV}, 0.60 \text{ GeV})$. This region has also been observed in Ref.[85] by comparing with the pQCD and LCSRs estimations at $Q^2 = 0$, $F_{+}^{B\pi}(0) = 0.258 \pm 0.031$ and $F_{+}^{B\pi}(0) = 0.253 \pm 0.028$ [87, 88]. This region can be further constrained by comparing $B \rightarrow K$ TFFs [85], i.e. as shown by Fig.(7), we obtain $\delta \sim (0.25, 0.30)$ and $\bar{\Lambda} \sim (0.50 \text{ GeV}, 0.55 \text{ GeV})$.

B. Determination of $|V_{cb}|$

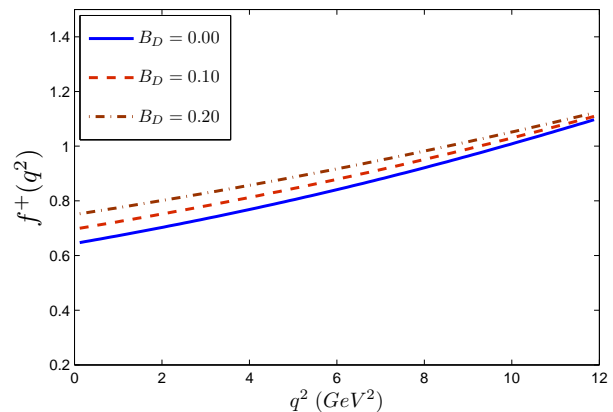


FIG. 8. The TFF $f^+(q^2)$ for D meson DA ϕ_D (29) with different choice of B [57]. The solid, the dashed and the dash-dot lines are for $B_D = 0.00, 0.10$ and 0.20 , respectively.

There are four $B \rightarrow D$ semi-leptonic processes that are frequently used to determine the CKM matrix element $|V_{cb}|$, i.e. $B^0 \rightarrow D^- \ell^+ \nu_\ell$, $\bar{B}^0 \rightarrow D^+ \ell^- \bar{\nu}_\ell$, $B^+ \rightarrow \bar{D}^0 \ell^+ \nu_\ell$ and $B^- \rightarrow D^0 \ell^- \bar{\nu}_\ell$. Schematically, we have

$$\frac{\mathcal{B}(B \rightarrow D \ell \bar{\nu}_\ell)}{\tau(B)} = \int_0^{(m_B - m_D)^2} dq^2 \frac{d\Gamma(B \rightarrow D \ell \bar{\nu}_\ell)}{dq^2}. \quad (27)$$

Here $\tau(B)$ stands for B meson lifetime and $\mathcal{B}(B \rightarrow D \ell \bar{\nu}_\ell)$ stands for the branching ratio of $B \rightarrow D \ell \bar{\nu}_\ell$, which are experimentally measurable. Under the limit $m_\ell \rightarrow 0$, the decay width takes the form [89, 90]

$$\frac{d\Gamma}{dq^2}(B \rightarrow D \ell \bar{\nu}_\ell) = \frac{G_F^2 |V_{cb}|^2}{192 \pi^3 m_B^3} \lambda^{\frac{3}{2}}(q^2) |f_+(q^2)|^2, \quad (28)$$

where $\lambda(q^2) = (m_B^2 + m_D^2 - q^2)^2 - 4m_B^2 m_D^2$ and $f_+(q^2)$ has been investigated by using several approaches, such as the lattice QCD [91], the pQCD [47] and the QCD LCSR [50, 57, 92–94]. Especially, a recent improved LCSR determination up to twist-4 accuracy has been presented in Ref.[57]. By using the improved LCSR with a chiral current correlator, the most uncertain twist-3 DAs make no contributions and twist-4 parts also provides small contributions about several percent, so the reliability of LCSR estimation can be enhanced to a large degree. This inversely makes the $B \rightarrow D$ semi-leptonic decays be good places for testing different models for the leading twist D meson LCDA. Based on the D meson WF modeled in the last section, we get its DA as,

$$\begin{aligned} \phi_D(x, \mu_0^2) = & \frac{A_D \sqrt{6x\bar{x}Y}}{8\pi^{3/2} f_D b_D} [1 + B_D C_2^{3/2}(x - \bar{x})] \times \\ & \exp \left[-b_D^2 \frac{xm_d^2 + \bar{x}m_c^2 - Y^2}{x\bar{x}} \right] \times \\ & \left[\text{Erf} \left(\frac{b_D \sqrt{\mu_0^2 + Y^2}}{\sqrt{x\bar{x}}} \right) - \text{Erf} \left(\frac{b_D Y}{\sqrt{x\bar{x}}} \right) \right] \end{aligned} \quad (29)$$

where A_D , B_D and b_D are undetermined parameters. The error function $\text{Erf}(x)$ is defined as $\text{Erf}(x) = 2 \int_0^x \exp(-t^2) dt / \sqrt{\pi}$, $Y = xm_d + \bar{x}m_c$ and $\bar{x} = 1 - x$. Some of its typical behaviors are presented in Fig.(4). The TFFs for ϕ_D with $B_D = 0.00, 0.10$ and 0.20 are presented in Fig.(8). It shows that $f^+(q^2)$ increases with the increment of B_D , which is consistent with the trends shown in Fig.(4) that a bigger B_D leads to a weaker suppression in the end-point region ($x \rightarrow 0$), and shall result in a larger estimation on $f^+(q^2)$.

B_D	B^0/\bar{B}^0 -type	B^\pm -type
0.00	$41.28^{+5.68}_{-4.82}$ $^{+1.13}_{-1.16}$	$40.44^{+5.56}_{-4.72}$ $^{+1.06}_{-1.09}$
0.10	$39.01^{+5.25}_{-4.59}$ $^{+1.06}_{-1.09}$	$38.22^{+5.14}_{-4.50}$ $^{+1.01}_{-1.03}$
0.20	$36.96^{+4.98}_{-4.43}$ $^{+1.01}_{-1.04}$	$36.21^{+4.88}_{-4.34}$ $^{+0.95}_{-0.98}$

TABLE III. The value of $|V_{cb}|$ in unit 10^{-3} [57]. The central values for $|V_{cb}|$ are obtained by setting all inputs to be their central values. The errors are calculated by theoretical and experimental errors on all inputs.

We discuss the variation of $|V_{cb}|$ by taking ϕ_D with several choices of B_D , in which the first (second) uncertainty comes from the squared average of the mentioned theoretical (experimental) uncertainties. The experimental uncertainty comes from the lifetime and the decay ratio of the mentioned processes [67]. The results are put in Table III. It is noted that the value of $|V_{cb}|$ decreases with the increment of B_D . The matrix element $|V_{cb}|$ and its uncertainties have been studied by using two types of processes, e.g. the B^0/\bar{B}^0 -type ($B^0 \rightarrow D^- \ell^+ \nu_\ell$ and $\bar{B}^0 \rightarrow D^+ \ell^- \bar{\nu}_\ell$) and the B^\pm -type ($B^+ \rightarrow \bar{D}^0 \ell^+ \nu_\ell$ and $B^- \rightarrow D^0 \ell^- \bar{\nu}_\ell$). For the case of $B_D=0$, by adding the errors from the ex-

perimental and theoretical uncertainty sources, we obtain $|V_{cb}|(B^0/\bar{B}^0 - \text{type}) = (41.28^{+6.81}_{-5.98}) \times 10^{-3}$ and $|V_{cb}|(B^\pm - \text{type}) = (40.44^{+6.54}_{-5.72}) \times 10^{-3}$. As a weighted average of these two types we obtain,

$$|V_{cb}| = (40.84 \pm 3.11) \times 10^{-3}, \quad (B_D = 0.00) \quad (30)$$

where the error stands for the standard derivation of the weighted average. Similarly, we have

$$|V_{cb}| = (39.08 \pm 3.03) \times 10^{-3}, \quad (B_D = 0.10), \quad (31)$$

$$|V_{cb}| = (37.59 \pm 2.89) \times 10^{-3}, \quad (B_D = 0.20). \quad (32)$$

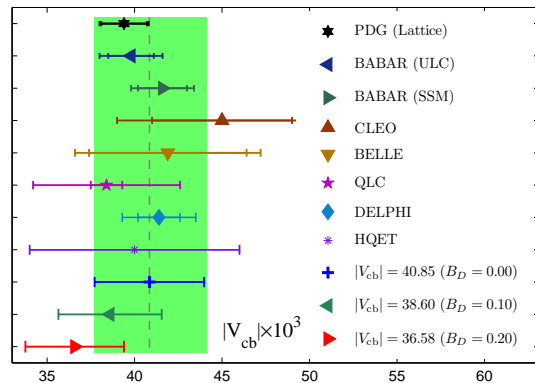


FIG. 9. A comparison of $|V_{cb}|$ with experimental and theoretical predictions [57]. Our estimations for $B_D = 0.00, 0.10$ and 0.20 are presented, where as a comparison, the results of BABAR [58], PDG (Lattice) [67], CLEO [60], Belle [59], QLC [91], DELPHI [95] and HQET [96] are also presented.

A comparison of $|V_{cb}|$ with experimental and theoretical predictions is put in Fig.(9), in which our estimations for $B_D = 0.00, 0.10$ and 0.20 are presented. Through a comparison with the experimental data, our present estimation for $|V_{cb}|$ shows a good agreement with the BABAR, CLEO and Belle estimates. It shows that to compare with the data, we need a small value for B_D .

C. Light meson-photon transition form factors

Firstly, we present the results for the pion-photon TFF. The pion-photon TFF provides the simplest example for the perturbative analysis to exclusive process [97]. To explain the abnormal large Q^2 behavior observed by the BABAR Collaboration in 2009 [98], many works have been done, e.g. by the pQCD [39, 40, 99, 100] or by LCSR [101–103]. However, last year, the Belle Collaboration released their new analysis [104], which dramatically different from those reported by BABAR Collaboration, but likely to agree with the asymptotic behavior estimated by Ref.[97]. Many attempts have been tried to clarify the situation [41, 105–109].

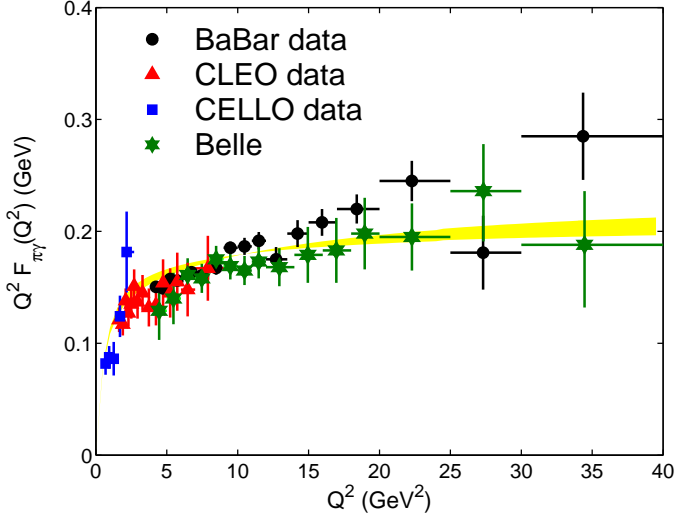


FIG. 10. $Q^2 F_{\pi\gamma}(Q^2)$ with our WF model (17,19) by varying the model parameter B_π within the region $[0.01, 0.14]$ [42]. The shaded band is our theoretical estimation. The experimental data are taken from Refs.[98, 104, 111–113].

Generally, the pion-photon TFF $F_{\pi\gamma}(Q^2)$ can be written as a sum of the valence quark part $F_{\pi\gamma}^{(V)}(Q^2)$ and the non-valence quark part $F_{\pi\gamma}^{(NV)}(Q^2)$ [39–41, 110]:

$$F_{\pi\gamma}(Q^2) = F_{\pi\gamma}^{(V)}(Q^2) + F_{\pi\gamma}^{(NV)}(Q^2). \quad (33)$$

The valence quark part $F_{\pi\gamma}^{(V)}(Q^2)$ indicates the pQCD calculable leading Fock-state contribution, which dominates the TFF when Q^2 is large. The non-valence quark part $F_{\pi\gamma}^{(NV)}(Q^2)$ is related to the non-perturbative higher Fock-states contributions, which can be estimated via a proper phenomenological model. Both the analytic expressions for $F_{\pi\gamma}^{(V)}(Q^2)$ and $F_{\pi\gamma}^{(NV)}(Q^2)$ can be found in Ref.[39].

Taking all input parameters to be the same as those adopted in Ref.[42], we draw the pion-photon TFF $F_{\pi\gamma}(Q^2)$ in Fig.(10). The upper and lower borderlines correspond to $B_\pi = 0.01$ and 0.14 respectively. It shows that in the small Q^2 region, $Q^2 \lesssim 15 \text{ GeV}^2$, the pion-photon TFF can explain the CELLO [111], CLEO [112, 113], BABAR [98] and Belle [104] experimental data simultaneously. While for the large Q^2 region, our present estimation favors the Belle data and disfavors the BABAR data. If taking $B_\pi \in [0.01, 0.42]$, the calculated curve for the pion-photon TFF with the upper limit of the parameter ($B_\pi = 0.42$) will be between the Belle and BABAR data. It is expected that BABAR and Belle can obtain more accurate and consistent data in the future, then the behavior of the pion DA can be further determined completely.

Secondly, we discuss the η - γ and η' - γ TFFs. Under the quark-flavor mixing scheme, the η - γ and η' - γ TFFs are related with $F_{\eta_q\gamma}(Q^2)$ and $F_{\eta_s\gamma}(Q^2)$ through the fol-

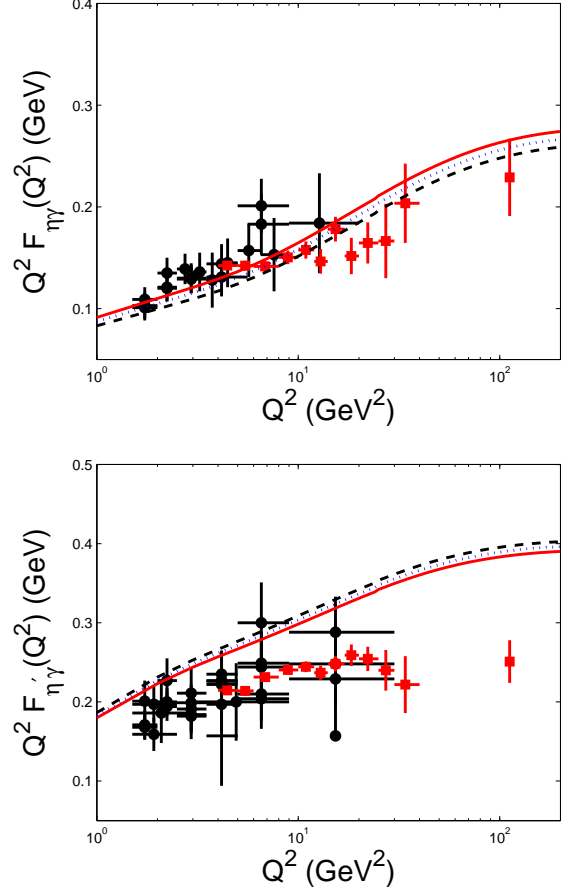


FIG. 11. η - γ and η' - γ TFFs $Q^2 F_{\eta\gamma}(Q^2)$ and $Q^2 F_{\eta'\gamma}(Q^2)$ with fixed $B_{\eta,\eta'} = 0.3$ and $m_q = 0.30 \text{ GeV}$ and $m_s = 0.45 \text{ GeV}$ [40]. The solid, the dotted and the dashed lines are for $\phi = 39.0^\circ$, 39.5° and 40.0° , respectively. The experimental data are taken from Refs.[112, 113, 117, 118].

lowing equations [40]

$$F_{\eta\gamma}(Q^2) = F_{\eta_q\gamma}(Q^2) \cos \phi - F_{\eta_s\gamma}(Q^2) \sin \phi \quad (34)$$

$$F_{\eta'\gamma}(Q^2) = F_{\eta_q\gamma}(Q^2) \sin \phi + F_{\eta_s\gamma}(Q^2) \cos \phi, \quad (35)$$

where ϕ is the mixing angle, which as a weighted average of experimental results [114–116], is about $39.5^\circ \pm 0.5^\circ$. Thus these two TFFs can also be adopted for determining the η_q and η_s WFs, which can be constructed in a similar way of pion WF. Due to η - η' mixing, we need to consider these two TFFs simultaneously. The curves of $Q^2 F_{\eta\gamma}(Q^2)$ and $Q^2 F_{\eta'\gamma}(Q^2)$ for $\phi = 39.5^\circ \pm 0.5^\circ$ are presented in Fig.(11). With the increment of m_q and m_s , the values of $Q^2 F_{\eta\gamma}(Q^2)$ and $Q^2 F_{\eta'\gamma}(Q^2)$ increase in lower Q^2 region and decrease in higher Q^2 region. And it is found that $Q^2 F_{\eta\gamma}(Q^2)$ decreases with the increment of ϕ , while $Q^2 F_{\eta'\gamma}(Q^2)$ increases with the increment of ϕ . By shifting ϕ to a smaller value $\sim 38^\circ$, one can explain them within $Q^2 < 20 \text{ GeV}^2$ consistently [119], which can not explain the newly BABAR data on η - γ and η' - γ for larger $Q^2 > 20 \text{ GeV}^2$. A proper intrinsic charm may have

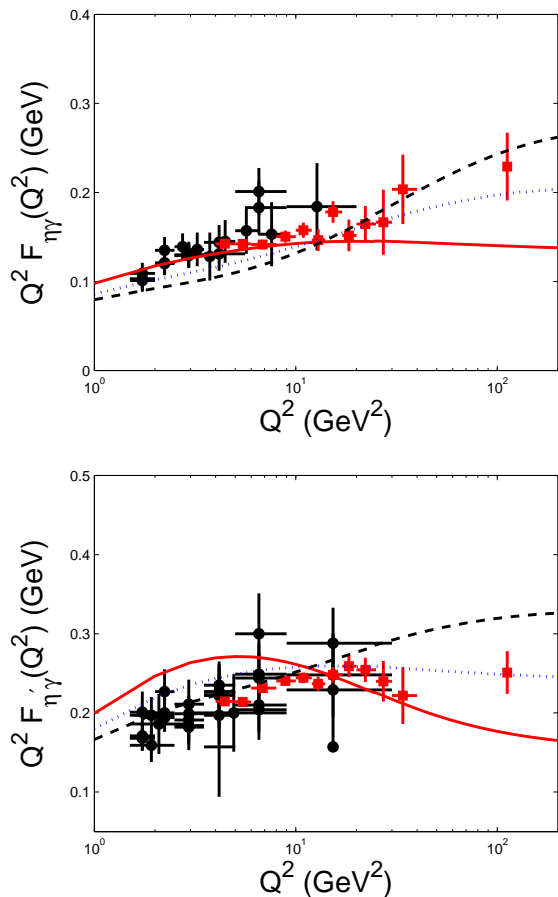


FIG. 12. η - γ and η' - γ TFFs $Q^2 F_{\eta\gamma}(Q^2)$ and $Q^2 F_{\eta'\gamma}(Q^2)$ [40], where $f_{\eta'}^c = -30$ MeV, $m_q = 0.30$ GeV, $m_s = 0.45$ GeV and $m_c = 1.50$ GeV. The solid, the dotted and the dashed lines are for $B_{\eta,\eta'} = 0.0, 0.30$ and 0.60 , respectively. The experimental data are taken from Refs.[112, 113, 117, 118].

some help to explain the abnormally large production of η' . It has been shown that the experimental data disfavors a larger portion of charm component as $|f_{\eta'}^c| \gtrsim 50$ MeV [40, 119].

More over, we present the results for η - γ and η' - γ TFFs with fixed $f_{\eta'}^c = -30$ MeV in Fig.(12), where $B_{\eta,\eta'} = 0.0, 0.30$ and 0.60 respectively. It shows that with proper charm component $f_{\eta'}^c \sim -30$ MeV and $B_{\eta,\eta'} \sim 0.30$, the experimental data on $Q^2 F_{\eta\gamma}(Q^2)$ and $Q^2 F_{\eta'\gamma}(Q^2)$ can be consistently explained. A moderate DA with $B_{\eta,\eta'} \sim 0.30$, corresponding to the second Gegenbauer DA moment around 0.35 for η_q and η_s DAs.

IV. SUMMARY AND OUTLOOK

The heavy and light meson WFs are nonperturbative but universal physical quantities in high energy processes and are important components for applying pQCD factorization theory. A better understanding of LCWF may

also be helpful for solving the factorization scale setting problem following the idea of the principle of maximum conformality to solve renormalization scale ambiguity [126–129]. In the present paper, we have reviewed recent progresses on constructing the B meson and light pseudoscalar WFs and have presented some of their applications. Those examples inversely provide some stringent constraints on determining the WF properties.

By taking the RG evolution effects into account, the heavy B meson WF is renormalizable and is an important component for the k_T factorization approach [18]. Under the WW approximation, its transverse and longitudinal momentum dependence is correlated through a simple δ -function, $\delta(\mathbf{k}_\perp^2 - \omega(2\bar{\Lambda} - \omega))$. While by including 3-particle Fock state, the transverse momentum distribution of the B meson WF is broadened to a hyperbola-like curve. The reasonable inclusion of the 3-particle Fock states in B meson WFs provides us with the chance to make a more precise evaluation on the B meson decays. By using the results derived from HQET, we provide a practical framework for constructing the B meson LC WFs $\Psi_\pm(\omega, z^2)$. Especially, we present a model in the compact parameter b -space. Its behaviors are controlled by two parameters $\bar{\Lambda}$ and δ . By taking $B \rightarrow \pi$ and $B \rightarrow K$ TFFs as an example, we show that if the 3-particle WFs' contributions are power suppressed than that of WW case, i.e. its contribution is less than 20%, then one obtains preferable values for these two parameters, $\delta \sim 0.27$ and $\bar{\Lambda} \sim 0.55$ GeV. In the literature, the $B \rightarrow \pi$ and $B \rightarrow K$ TFFs have been studied within the framework of LCSR [87, 88, 94, 120–125], a comparison of them with the pQCD estimation can also be adopted for constraining the B meson WF parameters. Further studies on the B meson WFs with higher Fock states and its phenomenological implications are still necessary.

We have suggested a revised light-cone harmonic oscillator model for the WFs of light mesons as $\pi, K, \eta^{(\prime)}, D$ and etc.. By using the constraint from the semi-leptonic process $B \rightarrow \pi l \nu$, the parameter B_π is restricted to be [0.01, 0.42]. If taking the process $D \rightarrow \pi l \nu$ as a further constraint, we can obtain a more narrow region $B_\pi = [0.00, 0.14]$ [42]. For the pion-photon TFF, our present result with the parameter $B_\pi = [0.01, 0.14]$ favors the Belle data and the corresponding pion DA has the slight difference from the asymptotic form. Then, one can predict the behavior of the pion-photon TFF in high Q^2 regions which can be tested in future experiments.

The $B \rightarrow D$ TFF up to twist-4 accuracy by using the improved QCD LCSR with chiral current provides a platform for testing the properties of twist-2 DA. Its second Gegenbauer moment is determined by the parameter B_D , $a_2^D \sim B_D$. By using a proper choice of B_D , most of the DA shapes suggested in the literature can be simulated. It is noted that to compare with the experimental result on $\mathcal{G}(1)|V_{cb}$, a smaller $B_D \lesssim 0.20$ shows a better agreement with the BABAR, CLEO and Belle estimates. By varying $B_D \in [0.00, 0.20]$, its first Gegenbauer moment a_1^D is about [0.6, 0.7]. The matrix element $|V_{cb}|$ and its

uncertainties have been studied by using two types of processes, e.g. the B^0/\bar{B}^0 -type and the B^\pm -type. For the case of $B_D = 0$, by adding the errors for all mentioned experimental and theoretical uncertainty sources, we obtain $|V_{cb}| = (40.84 \pm 3.11) \times 10^{-3}$, where the error stands for the standard derivation of the weighted average. Through a comparison with the experimental data, our present estimation for $|V_{cb}|$ shows a good agreement.

To test the properties of the constructed light pseudoscalar meson DAs, we have discussed the properties of the light pseudoscalar meson-photon TFFs, i.e. $\pi\text{-}\gamma$, $\eta\text{-}\gamma$ and $\eta'\text{-}\gamma$ TFFs. They provide good platforms for studying the DA of the light pseudoscalar mesons. The data from Belle and BABAR have a big difference on the $\pi\text{-}\gamma$ TFF in high Q^2 regions, at present, they are helpless for determining the pion DA. But it is still possible to determine the pion DA as long as we perform a combined analysis of the most existing data of the processes involving pion such as $\pi \rightarrow \mu\bar{\nu}$, $\pi^0 \rightarrow \gamma\gamma$, $B \rightarrow \pi l\nu$, $D \rightarrow \pi l\nu$, and etc. More over, we have shown that all pseudoscalar meson-photon transition form factors $Q^2 F_{\pi\gamma}(Q^2)$, $Q^2 F_{\eta\gamma}(Q^2)$ and $Q^2 F_{\eta_s\gamma}(Q^2)$ have sim-

ilar behaviors. No rapid growth has been observed for $Q^2 F_{\eta\gamma}(Q^2)$ and $Q^2 F_{\eta'\gamma}(Q^2)$, and these two TFFs can be simultaneously explained by setting $B_{\pi,\eta,\eta'} \sim 0.30$. Possible charm components f_η^c and $f_{\eta'}^c$ can shrink the gap between these two TFFs to a certain degree.

As a final remark, in addition to our present LCWF models for the pseudoscalar mesons, such BHL-like model can also be extended to higher twist LCWFs and the LCWFs for other light mesons as the scalars or vectors. In combination with a wide variety of exclusive or semi-exclusive processes involving light mesons, we hope the behaviors of the light mesons' LCWFs and hence their DAs can be determined via global fits of various experimental results finally.

Acknowledgments: This work was supported in part by Natural Science Foundation of China under Grant No.11075225, No.11275280 and No.11235005, by the Program for New Century Excellent Talents in University under Grant No.NCET-10-0882, and by the Fundamental Research Funds for the Central Universities under Grant No.CQDXWL-2012-Z002.

-
- [1] Brodsky SJ, Lepage GP (1981) Large angle two photon exclusive channels in quantum chromodynamics. Phys. Rev. D 24:1808-1817
 - [2] Brodsky SJ, Teramond GF (2013) QCD on the light-front - a systematic approach to hadron physics. arXiv: 1310.8648
 - [3] Georgi H (1990) An effective field theory for heavy quarks at low-energies. Phys. Lett. B 240:447-450
 - [4] Falk AF, Georgi H, Grinstein B et al (1990) Heavy meson form-factors from QCD. Nucl. Phys. B 343:1-13
 - [5] Neubert M (1994) Heavy quark symmetry. Phys. Rept. 245:259-396
 - [6] Guo XH, Huang T (1991) Hadronic wave functions in D and B decays. Phys. Rev. D 43:2931-2938
 - [7] Beneke M, Feldmann T (2001) Symmetry breaking corrections to heavy to light B meson form-factors at large recoil. Nucl. Phys. B 592:3-34
 - [8] Genon SD, and Sachrajda CT (2002) Sudakov effects in $B \rightarrow \pi l \nu(l)$ form-factors. Nucl. Phys. B 625:239-278
 - [9] Lange BO, Neubert M (2003) Renormalization group evolution of the B meson light cone distribution amplitude. Phys. Rev. Lett. 91:102001
 - [10] Lee SJ and Neubert M (2005) Model-independent properties of the B-meson distribution amplitude. Phys. Rev. D 72:094028
 - [11] Geyer B, Witzel O (2005) B-meson distribution amplitudes of geometric twist vs. dynamical twist. Phys. Rev. D 72:034023
 - [12] Khodjamirian A, Mannel T, Offen N (2005) B-meson distribution amplitude from the $B \rightarrow \pi$ form-factor. Phys. Lett. B 620:52-60
 - [13] Braun VM, Ivanov DY, Korchemsky GP (2004) The B meson distribution amplitude in QCD. Phys. Rev. D 69:034014
 - [14] Geyer B, Witzel O (2007) Heavy meson distribution amplitudes of definite geometric twist with contribution of 3-particle distribution amplitudes. Phys. Rev. D 76:074022
 - [15] Bell G, Feldmann T (2008) Modelling light-cone distribution amplitudes from non-relativistic bound states. J. High Energy Phys. 0804:061
 - [16] Kawamura H, Tanaka K (2010) Evolution equation for the B-meson distribution amplitude in the heavy-quark effective theory in coordinate space. Phys. Rev. D 81:114009
 - [17] Bell G, Feldmann T, Wang YM et al (2013) Light-cone distribution amplitudes for heavy-quark hadrons. J. High Energy Phys. 1311:191
 - [18] Li HN, Liao HS (2004) B meson wave function in k(T) factorization. Phys. Rev. D 70:074030
 - [19] Kawamura H, Kodaira J, Qiao CF et al (2001) B meson light cone distribution amplitudes in the heavy quark limit. Phys. Lett. B 523:111-116
 - [20] Kawamura H, Kodaira J, Qiao CF et al (2003) Transverse momentum distribution in B mesons in the heavy quark limit: The Wandzura-Wilczek part. Mod. Phys. Lett. A 18:799-805
 - [21] Huang T, Wu XG, Zhou MZ (2005) B-meson wavefunction in the Wandzura-Wilczek approximation. Phys. Lett. B 611:260-268
 - [22] Huang T, Qiao CF, Wu XG (2006) B-meson wave function with contributions from three-particle Fock states. Phys. Rev. D 73:074004
 - [23] Isgur N, Wise MB (1989) Weak decays of heavy mesons in the static quark approximation. Phys. Lett. B 232:113-117
 - [24] Isgur N, Wise MB (1990) Weak transition form-factors between heavy mesons. Phys. Lett. B 237:527-530
 - [25] Eichten E, Hill BR (1990) An effective field theory for the calculation of matrix elements involving heavy

- quarks. Phys. Lett. B 234:511-516
- [26] Wandzura S, Wilczek F (1977) Sum rules for spin dependent electroproduction: test of relativistic constituent quarks. Phys. Lett. B 72:195-198
- [27] Brodsky SJ, Huang T, Lepage GP (1983) Hadronic wave functions and high momentum transfer interactions in quantum chromodynamics. In: Capri AZ, Kamal AN (ed) Particles and Fields-2 - Proceedings, New York, Plenum Press, pp 143-199
- [28] Lepage GP, Brodsky SJ, Huang T, Mackenzie PB (1983) Hadronic wave functions in QCD. In: Capri AZ, Kamal AN (ed) Particles and Fields-2 - Proceedings, New York, Plenum Press, pp 83-116
- [29] Huang T (1981) Hadron Wave Functions and Structure Functions in QCD. In: Durand L, Pondrom LG (ed) High energy physics - 1980: proceedings, New York, Amer. Inst. Phys., pp 1000-1004
- [30] Huang T, Ma BQ, Shen QX (1994) Analysis of the pion wave function in light cone formalism. Phys. Rev. D 49:1490-1499
- [31] Cao FG, Huang T (1999) Large corrections to asymptotic $F(\eta_c \gamma)$ and $F(\eta_b \gamma)$ in the light cone perturbative QCD. Phys. Rev. D 59:093004
- [32] Huang T, Wu XG, Wu XH (2004) Pion form-factor in the $k(T)$ factorization formalism. Phys. Rev. D 70:053007
- [33] Wu XG, Huang T (2006) Pion electromagnetic form-factor in the $K(T)$ factorization formulae. Int. J. Mod. Phys. A 21:901-904
- [34] Huang T, Wu XG (2004) A model for the twist-3 wave function of the pion and its contribution to the pion form-factor. Phys. Rev. D 70:093013
- [35] Wu XG, Huang T (2008) kaon electromagnetic form-factor within the $k(T)$ factorization formalism and its light-cone wave function. J. High Energy Phys. 0804:043
- [36] Cao FG, Huang T, Ma BQ (1996) The perturbative pion - photon transition form-factors with transverse momentum corrections. Phys. Rev. D 53:6582-6585
- [37] Cao FG, Cao J, Huang T et al (1997) The hard scattering amplitude for the higher helicity components of the pion form-factor. Phys. Rev. D 55:7107-7113
- [38] Xiao BW, Ma BQ (2003) Pion photon and photon pion transition form-factors in the light cone formalism. Phys. Rev. D 68:034020
- [39] Wu XG, Huang T (2010) An implication on the pion distribution amplitude from the pion-photon transition form factor with the new BABAR data. Phys. Rev. D 82:034024
- [40] Wu XG, Huang T (2011) Constraints on the light pseudoscalar meson distribution amplitudes from their meson-photon transition form factors. Phys. Rev. D 84:074011
- [41] Wu XG, Huang T, Zhong T (2013) Information on the pion distribution amplitude from the pion-photon transition form factor with the Belle and BaBar data. Chin. Phys. C 37:063105
- [42] Huang T, Zhong T, Wu XG (2013) Determination of the pion distribution amplitude. Phys. Rev. D 88:034013
- [43] Brodsky SJ, Cao FG, Teramond GF (2011) Evolved QCD predictions for the meson-photon transition form factors. Phys. Rev. D 84:033001
- [44] Brodsky SJ, Cao FG, Teramond GF (2011) Meson transition form factors in light-front holographic QCD. Phys. Rev. D 84:075012
- [45] Cao FG, Huang T, Luo CW (1995) Reexamination of the perturbative pion form-factor with Sudakov suppression. Phys. Rev. D 52, 5358-5361
- [46] Chernyak VL, Zhitnitsky AR (1982) Exclusive decays of heavy mesons. Nucl. Phys. B 201:492-526
- [47] Kurimoto T, Li HN, Sanda AI (2003) $B \rightarrow D^{(*)}$ form-factors in perturbative QCD. Phys. Rev. D 67:054028
- [48] Bondar AE, Chernyak VL (2005) Is the BELLE result for the cross section $\sigma(e^+ e^- \rightarrow J/\psi + \eta_c)$ a real difficulty for QCD? Phys. Lett. B 612:215-222
- [49] Braguta VV, Likhoded AK, Luchinsky AV (2007) The Study of leading twist light cone wave function of η_c meson. Phys. Lett. B 646:80-90
- [50] Zuo F, Huang T (2007) $B_c(B) \rightarrow D\ell\bar{\nu}$ form-factors in light-cone sum rules and the D meson distribution amplitude. Chin. Phys. Lett. 24:61-64
- [51] Huang T, Zuo F (2007) Semileptonic B_c decays and charmonium distribution amplitude. Eur. Phys. J. C 51:833-839
- [52] Sun YJ, Wu XG, Zuo F et al (2010) The Cross section of the process $e^+ + e^- \rightarrow J/\psi + \eta_c$ within the QCD light-cone sum rules. Eur. Phys. J. C 67:117-123
- [53] Ma JP, Si ZG (2007) NRQCD factorization for twist-2 light-cone wave-functions of charmonia. Phys. Lett. B 647:419-426
- [54] Braguta VV (2007) The study of leading twist light cone wave functions of J/ψ meson. Phys. Rev. D 75:094016
- [55] Hwang CW (2009) Study of quark distribution amplitudes of 1S and 2S heavy quarkonium states. Eur. Phys. J. C 62:499-509
- [56] Braguta VV, Likhoded AK, Luchinsky AV (2012) Exclusive processes of charmonium production and charmonium wave functions. Phys. Atom. Nucl. 75:97-108
- [57] Fu HB, Wu XG, Han HY et al (2013) V_{cb} from the semileptonic decay $B \rightarrow D\ell\bar{\nu}_\ell$ and the properties of the D meson distribution amplitude. arXiv:1309.5723
- [58] Aubert B et al (BABAR Collaboration) (2010) Measurement of $|V_{cb}|$ and the form-factor slope in anti- $b \rightarrow d$ l - anti- ν decays in events tagged by a fully reconstructed B meson. Phys. Rev. Lett. 104:011802
- [59] Abe K et al (Belle Collaboration) (2002) Measurement of $B(\text{anti-}B_0 \rightarrow D^+ l^- \text{anti-}\nu)$ and determination of $|V_{cb}|$. Phys. Lett. B 526:258-268
- [60] Bartelt J et al (CLEO Collaboration) (1999) Measurement of the $B \rightarrow D$ lepton neutrino branching fractions and form-factor. Phys. Rev. Lett. 82:3746
- [61] Grozin AG, Neubert M (1997) Asymptotics of heavy meson form-factors. Phys. Rev. D 55:272-290
- [62] Halperin IE, Zhitnitsky A (1997) Hard diffractive electroproduction, transverse momentum distribution and QCD vacuum structure. Phys. Rev. D 56:184-197
- [63] Botts J, Sterman G (1989) Hard Elastic Scattering in QCD: Leading Behavior. Nucl. Phys. B 325:62-100
- [64] Huang T, Shen QX (1991) A study of the applicability of perturbative QCD to the pion form-factor. Z. Phys. C 50:139-144
- [65] Li HN, Sterman G (1992) The Perturbative pion form-factor with Sudakov suppression. Nucl. Phys. B 381:129-140
- [66] Nagashima M, Li HN (2003) $k(T)$ factorization of exclusive processes. Phys. Rev. D 67:034001
- [67] Beringer J et al (Particle Data Group) (2012) Review of particle physics. Phys. Rev. D 86:010001
- [68] Bodwin GT, Kang D, Lee J (2006) Reconciling the light-

- cone and NRQCD approaches to calculating $e^+ e^- \rightarrow J/\psi + \eta(c)$. Phys. Rev. D 74:114028
- [69] Braguta VV, Likhoded AK, Luchinsky AV (2007) The study of leading twist light cone wave function of $\eta(c)$ meson. Phys. Lett. B 646:80-90
- [70] Xiao BW, Qian X, Ma BQ (2002) The kaon form-factor in the light cone quark model. Eur. Phys. J. A 15:523-527
- [71] Choi HM, Ji CR (2006) Conformal symmetry and pion form-factor: soft and hard contributions. Phys. Rev. D 74:093010
- [72] Ji CR, Chung PL, Cotanch SR (1992) Light cone quark model axial vector meson wave function. Phys. Rev. D 45:4214-4220
- [73] Choi HM, Ji CR (2007) Distribution amplitudes and decay constants for (π, K, ρ, K^*) mesons in light-front quark model. Phys. Rev. D 75:034019
- [74] Ball P, Braun VM, Lenz A (2006) Higher-twist distribution amplitudes of the K meson in QCD. J. High Energy Phys. 0605:004
- [75] Khodjamirian A, Mannel T, Melcher M (2004) Kaon distribution amplitude from QCD sum rules. Phys. Rev. D 70:094002
- [76] Ball P, Boglione M (2003) SU(3) breaking in K and K^* distribution amplitudes. Phys. Rev. D 68:094006
- [77] Braun VM, Lenz A (2004) On the SU(3) symmetry-breaking corrections to meson distribution amplitudes. Phys. Rev. D 70:074020
- [78] Ball P, Zwicky R (2006) Operator relations for SU(3) breaking contributions to K and K^* distribution amplitudes. J. High Energy Phys. 0602:034
- [79] Boyle PA et al (UKQCD Collaboration) (2006) A Lattice Computation of the First Moment of the Kaon's Distribution Amplitude. Phys. Lett. B 641:67-74
- [80] Braun VM et al (QCDSF/UKQCD Collaboration) (2006) Moments of pseudoscalar meson distribution amplitudes from the lattice. Phys. Rev. D 74:074501
- [81] Nam S, Kim HC (2006) Leading-twist pion and kaon distribution amplitudes in the gauge-invariant nonlocal chiral quark model from the instanton vacuum. Phys. Rev. D 74:076005
- [82] Chernyak VL, Zhitnitsky AR (1984) Asymptotic Behavior of Exclusive Processes in QCD. Phys. Rep. 112:173-318
- [83] Chernyak VL, Zhitnitsky AR (1984) Nucleon wave function and nucleon form-factors in QCD. Nucl. Phys. B 246:52-74
- [84] Huang T, Wu XG (2005) Consistent calculation of the B to pi transition form-factor in the whole physical region. Phys. Rev. D 71:034018
- [85] Zeng DM, Wu XG, Fang ZY (2009) B-meson wave function through a comparative analysis of the $B \rightarrow \pi, K$ transition form factors. Chin. Phys. Lett. 26:021401
- [86] Charng YY, Li HN (2005) B meson wave function from the $B \rightarrow \gamma l \nu$ decay. Phys. Rev. D 72:014003
- [87] Ball P, Zwicky R (2005) New results on $B \rightarrow \pi, K, \eta$ decay formfactors from light-cone sum rules. Phys. Rev. D 71:014015
- [88] Ball P (2007) $|V(\text{ub})|$ from UTangles and $B \rightarrow \pi l \nu$. Phys. Lett. B 644:38-44
- [89] Khodjamirian A, Rückl R (1998) QCD sum rules for exclusive decays of heavy mesons. Adv. Ser. Direct. High Energy Phys. 15:345-401
- [90] Ball P, Zwicky R (2005) $|V(\text{ub})|$ and constraints on the leading-twist pion distribution amplitude from $B \rightarrow \pi l \nu$. Phys. Lett. B 625:225-233
- [91] Divitiis GM, Molinaro E, Petronzio R et al (2007) Quenched lattice calculation of the $B \rightarrow D l \nu$ decay rate. Phys. Lett. B 655:45-49
- [92] Zuo F, Li ZH, Huang T (2006) Form factor for $B \rightarrow D l \nu$ in light-cone sum rules with chiral current correlator. Phys. Lett. B 641:177-182
- [93] Kurimoto T, Li HN, Sanda AI (2003) $B \rightarrow D^{(*)}$ form-factors in perturbative QCD. Phys. Rev. D 67:054028
- [94] Huang T, Li ZH, Wu XY (2001) Improved approach to the heavy to light form-factors in the light cone QCD sum rules. Phys. Rev. D 63:094001
- [95] Abdallah J et al (DELPHI Collaboration) (2004) Measurement of $|V(\text{cb})|$ using the semileptonic decay $\text{anti-B}0(d) \rightarrow D^{*+} l^- \text{anti-}\nu(l)$. Eur. Phys. J. C 33:213-232
- [96] Albertus C, Hernandez E, Nieves J et al (2005) Study of the leptonic decays of pseudoscalar B, D and vector B^*, D^* mesons and of the semileptonic $B \rightarrow D$ and $B \rightarrow D^*$ decays. Phys. Rev. D 71:113006
- [97] Lepage GP, Brodsky SJ (1980) Exclusive processes in perturbative quantum chromodynamics. Phys. Rev. D 22:2157-2198
- [98] Aubert B et al (BABAR Collaboration) (2009) Measurement of the $\gamma \gamma^* \rightarrow \pi^0$ transition form factor. Phys. Rev. D 80:052002
- [99] Noguera S, Vento V (2010) The pion transition form factor and the pion distribution amplitude. Eur. Phys. J. A 46:197-205
- [100] Kroll P (2011) The form factors for the photon to pseudoscalar meson transitions - an update. Eur. Phys. J. C 71:1623
- [101] Mikhailov SV, Stefanis NG (2009) Transition form factors of the pion in light-cone QCD sum rules with next-to-next-to-leading order contributions. Nucl. Phys. B 821:291-326
- [102] Bakulev AP, Mikhailov SV, Pimikov AV et al (2011) Pion-photon transition: The New QCD frontier. Phys. Rev. D 84:034014
- [103] Agaev SS, Braun VM, Offen N et al (2011) Light cone sum rules for the π^0 - γ^* - γ form factor revisited. Phys. Rev. D 83:054020
- [104] Uehara S et al (Belle Collaboration) (2012) Measurement of $\gamma \gamma^* \rightarrow \pi^0$ transition form factor at Belle. Phys. Rev. D 86:092007
- [105] Agaev SS, Braun VM, Offen N et al (2012) BELLE Data on the $\pi^0 \gamma^* \gamma$ Form Factor: A Game Changer? Phys. Rev. D 86:077504
- [106] Bakulev AP, Mikhailov SV, Pimikov AV et al (2012) Comparing antithetic trends of data for the pion-photon transition form factor. Phys. Rev. D 86:031501
- [107] Noguera S, Vento V (2012) Model analysis of the world data on the pion transition form factor. Eur. Phys. J. A 48:143
- [108] Stefanis NG, Bakulev AP, Mikhailov SV et al (2013) Can we understand an auxetic pion-photon transition form factor within QCD? Phys. Rev. D 87:094025
- [109] Huang T, Wu XG, Zhong T (2013) Finding a way to determine the pion distribution amplitude from the experimental data. Chin. Phys. Lett. 30:041201
- [110] Huang T, Wu XG (2007) A comprehensive analysis on the pion-photon transition form factor involving the transverse momentum corrections. Int. J. Mod. Phys. A 22:3065-3086

- [111] Behrend HJ et al (CELLO Collaboration) (1991) A measurement of the π^0 , η and η' electromagnetic form-factors. *Z. Phys. C* 49:401-410
- [112] Savinov V et al (CLEO Collaboration) (1997) Measurements of the meson - photon transition form-factors of light pseudoscalar mesons at large momentum transfer. hep-ex/9707028.
- [113] Gronberg J et al (CLEO Collaboration) (1998) Measurements of the meson - photon transition form-factors of light pseudoscalar mesons at large momentum transfer. *Phys. Rev. D* 57:33-54
- [114] Feldmann T, Kroll P, Stech B (1998) Mixing and decay constants of pseudoscalar mesons. *Phys. Rev. D* 58:114006
- [115] Kroll P (2005) Isospin symmetry breaking through π^0 - η - η' mixing. *Mod. Phys. Lett. A* 20:2667-2684
- [116] Ablikim M et al (BES Collaboration) (2006) Measurement of the branching fractions for $J/\psi \rightarrow \gamma \pi^0$, $\gamma \eta$ and $\gamma \eta'$. *Phys. Rev. D* 73:052008
- [117] Aubert B et al (BABAR Collaboration) (2006) Measurement of the η and η' transition form-factors at $q^2 = 112\text{-GeV}^2$. *Phys. Rev. D* 74:012002
- [118] Sanchez P et al (BABAR Collaboration) (2011) Measurement of the $\gamma \gamma^* \rightarrow \eta$ and $\gamma \gamma^* \rightarrow \eta'$ transition form factors. *Phys. Rev. D* 84:052001
- [119] Huang T, Wu XG (2007) Determination of the η and η' mixing angle from the pseudoscalar transition form factors. *Eur. Phys. J. C* 50:771-779
- [120] Wu XG, Huang T, Fang ZY (2008) SU(3)-symmetry breaking effects of the $B \rightarrow K$ transition form-factor in the QCD light-cone sum rules. *Phys. Rev. D* 77:074001
- [121] Wu XG, Huang T (2009) Radiative corrections on the $B \rightarrow P$ form factors with chiral current in the light-cone sum rules. *Phys. Rev. D* 79:034013
- [122] Li ZH, Zhu N, Fan XJ et al (2012) Form factors $f_+^{B \rightarrow \pi}(0)$ and $f_+^{D \rightarrow \pi}(0)$ in QCD and determination of $|V_{ub}|$ and $|V_{cb}|$. *J. High Energy Phys.* 1205:160
- [123] Huang T, Li ZH, Zuo F (2009) Heavy-to-light transition form factors and their relations in light-cone QCD sum rules. *Eur. Phys. J. C* 60:63-71
- [124] Duplancic G, Khodjamirian A, Mannel T et al (2008) Light-cone sum rules for $B \rightarrow \pi$ form factors revisited. *J. High Energy Phys.* 0804:014
- [125] Wang ZG, Zhou MZ, Huang T (2003) $B \pi$ weak form-factor with chiral current in the light cone sum rules. *Phys. Rev. D* 67:094006
- [126] Brodsky SJ, Wu XG (2012) Scale setting using the extended renormalization group and the principle of maximum conformality: the QCD coupling constant at four loops. *Phys. Rev. D* 85:034038
- [127] Brodsky SJ, Wu XG (2012) Eliminating the Renormalization Scale Ambiguity for Top-Pair Production Using the Principle of Maximum Conformality. *Phys. Rev. Lett.* 109:042002
- [128] Mojaza M, Brodsky SJ, Wu XG (2013) A systematic all-orders method to eliminate renormalization-scale and scheme ambiguities in pQCD. *Phys. Rev. Lett.* 110:192001
- [129] Wu XG, Brodsky SJ, Mojaza M (2013) The renormalization scale-setting problem in QCD. *Prog. Part. Nucl. Phys.* 72:44-98